Materials Science of the Gel to Fluid Phase Transition in a Supported Phospholipid Bilayer

Anne Feng Xie, Ryo Yamada, Andrew A. Gewirth,* and Steve Granick†

Departments of Chemistry, Materials Science and Engineering, and Frederick Seitz Materials Research Laboratory, University of Illinois, Urbana, Illinois 61801

(Received 23 May 2002; published 21 November 2002)

We report the results of *in situ* AFM measurements examining the phase transition of bilayers formed from the zwitterionic phospholipid, DMPC, 1,2-dimyristoyl-*sn*-glycero-3-phosphocholine, supported on mica. The images show that the fluid to gel phase transition process features substantial tearing of the bilayer due to the density change between the two phases. The gel to fluid transition is strongly affected by the resultant stress introduced into the gel phase, which changes the degree of cooperativity, the shape of developing fluid phase regions, and the course of the transition.

DOI: 10.1103/PhysRevLett.89.246103 PACS numbers: 68.37.Ps, 87.14.Cc

There is burgeoning use of supported lipid bilayers on planar substrates [1–10]. First, they provide model systems to study different physical phenomena on 2D surfaces with the advantage of a well-defined planar geometry. Second, on the practical side, they provide an environment in which to study polypeptides and membrane proteins [1–6]. In the "liquid-crystalline" (LC) phase, lipids display fluidity similar to that found in freestanding liposomes owing to the presence of a thin, lubricating water layer between the bilayers and the hard solid substrate [2]. Many phospholipid bilayers also display a first-order phase transition in the vicinity of room temperature to a lower-temperature "gel" phase in which lipid molecules within the bilayer are localized in space and the lipid tails have crystalline order [7].

In this Letter we quantify, using AFM (atomic force microscopy), how the microstructure of a simple class of these films evolves during the phase transformation process. The main new point is to show, for the first time to the best of our knowledge, that the gel to fluid transition is strongly affected by the resultant stress introduced into the gel phase. These questions of materials science — of defects and property changes introduced by processing — change the degree of cooperativity, the shape of developing fluid phase regions, and the course of the transition.

For study, we selected the zwitterionic phospholipid, DMPC, 1,2-dimyristoyl-*sn*-glycero-3-phosphocholine (Avanti Polar Lipids, Inc.), whose phase transition at 23–24 °C [7] affords convenient study of these bilayers at temperatures both below and above the phase transition temperature. The matched sizes of the polar headgroup and the lipid tail, combined with the absence of net electric charge in the headgroup, are known to enable the formation of planar bilayers of good quality [11]. AFM experiments were carried out with a PicoSPM 300 (Molecular Imaging) controlled with Nanoscope E controller (Digital Instruments). Images were acquired in Magnetic AC (MAC) mode [12], a noncontact method ideal for imaging delicate structures. The cantilever oscillation frequency was ca. 22 kHz and its spring constant was 2.8 N/m. A freshly cleaved sheet of muscovite mica was placed in an AFM liquid cell made of Teflon and sealed to the cell using a fluorocarbon O-ring. Temperature was controlled by using a reservoir of ice and an incandescent lamp to, respectively, gradually cool and heat the AFM chamber. The temperature was measured using a thermocouple placed just beneath the AFM sample stage.

Bilayers of DMPC were prepared by vesicle fusion using an adaptation of methods described elsewhere [1]. First, the DMPC was dissolved in chloroform and dried under a stream of N_2 followed by evacuation. Second, the dried lipid film was hydrated at 40 °C for at least 2 h and then mixed in a vortexer. Next, the hydrated lipids were subjected to five freeze/thaw cycles to produce small vesicles. Finally, small unilamellar vesicles were produced by extrusion 11 times through a pair of 100 nm pore size polycarbonate membranes. These were injected into the thermostatted AFM cell, incubated at 40 °C for at least 2 h to encourage equilibration; then excess unfused vesicles were rinsed out by copiously flushing the cell with phosphate solution buffered at $p\mathrm{H} = 6.0$. Most of the bilayer images taken of the fluid phase were free of defects with the areal percentage of defects well below 1% [Fig. 3(f)]. After cooling to the gel phase, big, foam-like defects were observed (Fig. 1). The defects extended to the mica substrate, giving the thickness of the bilayer —4.5 ± 1 nm, in good agreement with known values [8,10]. In addition, the height difference between the fluid and gel phases, 0.6 ± 0.2 nm, was slightly higher than the known value of 0.3–0.4 nm measured by neutron reflection [13].

Figures 1(a)–1(e) illustrate the fluid to gel phase transition process with decreasing temperature. The equilibration time at each temperature was ≈ 9 min. The fluid phase persisted until 21 °C, which is 2–3° lower than the phase transition temperature, likely due to supercooling. The sudden appearance of the gel phase ($> 60\%$ of the bilayer), which can be easily resolved from the fluid phase by the 0.6 ± 0.2 nm height increase on cooling, was

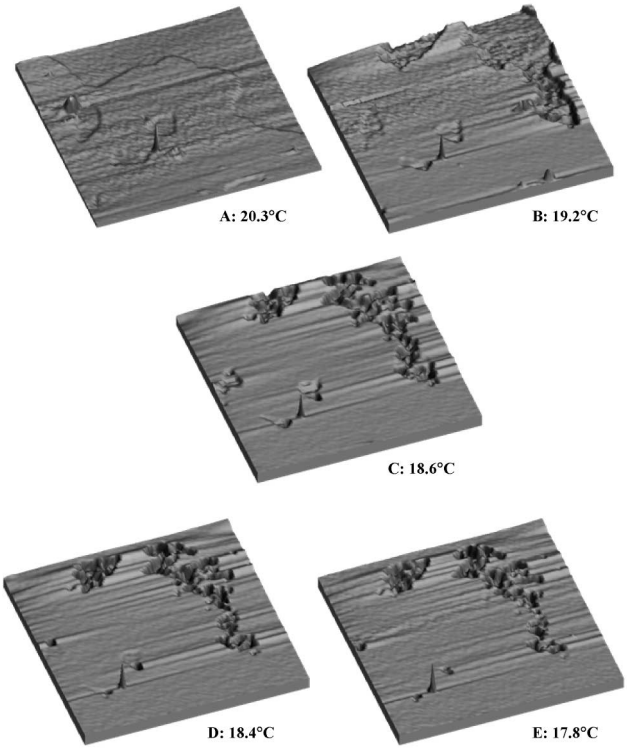

FIG. 1. Images of DMPC supported bilayer at 20.3 °C (a), 19.2 °C (b), 18.6 °C (c), 18.4 °C (d), and 17.8 °C (e) as the temperature was decreased from 26 °C to 17 °C. In each panel, the image area is 10 μm × 10 μm.

observed at 20.3 °C [Fig. 1(a)]. Note that in Fig. 1(a), the gel phase is a large area with small fluid domains isolated inside, indicating that the gel phase grew in a correlated process.

Figures 1(b)–1(d) show that as the gel phase continued to form, a large defect developed, as seen in the upper right of the image. The fluid bilayer was apparently torn on cooling, likely because of the different densities of the fluid and gel phases. As the bilayer was cooled through the transition, the thickness of the bilayer increased by 15%–20% due to the ordering of the hydrocarbon tails [14]. Since the volume density decreases about 3%–4% between the fluid and gel phases, it follows that the area per lipid molecule decreases about 15%–20% [15]. The defect density in Fig. 1 is on the order of 5%–7%, which is somewhat smaller than the 15%–20% expected. The origin of this discrepancy could be residual stress remaining in the gel phase, or more likely the presence of additional, large defects outside the imaging area.

Figures 1(b)–1(e) show that a small amount of fluid phase remained at even lower temperatures. As these finally transformed to the gel phase, a new type of defect formed in the bilayer, visible as holes in the lower left of Fig. 1(e). Tentatively, we attribute the persistence of the fluid phase at low temperatures to the difficulty of forming strain-relieving defects in the isolated supercooled fluid islands. Eventually, the bilayer surface displayed uniformly the gel phase but with stable, foamlike defects.

Figures 2(a)–2(c) display a more detailed view of the defect evolution. Interestingly, these defects appeared to heal with decreasing temperature. The area occupancy of defect decreased from 20% to 4% as the temperature was lowered from 19 to 18 °C. Figure 2(a) exhibits three regions with different heights. The lightest region (i) is the ordered, gel phase, while the darkest region (iii) is the holes created during the tearing process. The region in medium color (ii) is higher than the holes and lower than the gel phase by 2.7 nm and 1.6 nm, respectively. As the defects developed, the height difference between (i) and (ii) decreased until region (ii) appeared to join the gel phase in region (i). The defect area was now considerably less than originally at higher temperature. The variable height difference between (i) and (ii) indicates that region (ii) is not simply remaining a fluid phase, but rather is likely a disordered mobile phase whose density was lowered by tearing.

Thus initial tearing of the bilayer appeared to produce not empty space but instead a low density of lipid. Indeed, the depth of region (iii) was highly variable [see Figs. 2(a) and 2(b)]. As the temperature was lowered, these lipid molecules appeared to migrate to the defect edges and began to assemble into the gel phase, until at the lowest temperatures this process was completed [Fig. 2(c)]. Disorder should diminish as the temperature is lowered. The defect annealing process reported here underscores the mobility of the lipid material, even at relatively low temperatures.

Figure 3 is a series of AFM images showing the reverse process, the gel to fluid phase transition. Samples for melting were prepared by rapid quenching to 14 °C, unlike the slow freezing process detailed above. This rapid quenching undoubtedly afforded less time for lipids to migrate to the defect walls, leaving the circular foamlike features. Below 19 °C, defects tended to form a stable, continuous, foamlike structure [Fig. 3(a)], similar to Fig. 1(e), but more "foamy." Upon raising the temperature, annealing began: individual globules migrated to the edges of the defects and incorporated into the gel phase [Fig. 3(b)], leading to a decrease in the perimeter of the defects. This annealing was akin to Ostwald ripening.

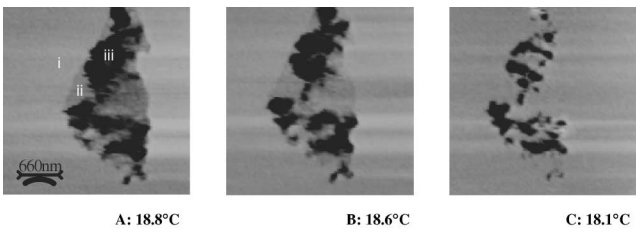

FIG. 2. Images of DMPC supported bilayer at 18.8 °C (a), 18.6 °C (b), and 18.1 °C (c), showing the evolution of defects in the course of the fluid to gel phase transition.

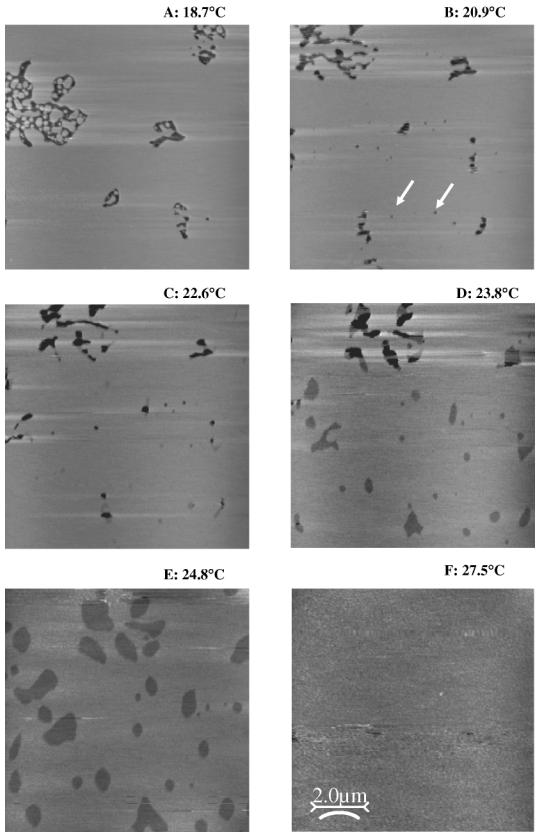

FIG. 3. Images of DMPC supported bilayer at 18.7 °C (a), 20.9 °C (b), 22.6 °C (c), 23.8 °C (d), 24.8 °C (e), and 27.5 °C (f) when raising the temperature from 14 °C to 28 °C. In each panel, the image area is 10 μm $\times$ 10 μm.

Above 20 °C, numerous small spots appeared in the gel phase [Fig. 3(b)]. Their shape was irregular and they served as nuclei for the gel to fluid phase transition. Interestingly, these nuclei did not form at the site of the preexisting defects. Because of the finite size of the AFM tip, the depth and size of the "fluid nuclei" cannot be quantified accurately, but it is clear that at sizes <0.01 μm^2, these nuclei were much smaller than the preexisting defects. Domains of the high-temperature phase were imaged even below 24 °C, but their area fraction was $<5\%$.

Figure 3(c) shows that the fluid phase grew from these fluid nuclei. As they grew, small spots of fluid phase also emerged at the periphery of the preexisting defects. Consequently, the fluid phase features substantially increased in size and number [Fig. 3(d)], and the perimeter of the fluid phase, i.e., the length of the interfacial boundary, also increased. At 24 °C, the amount of fluid phase began to grow rapidly and all traces of preexisting defects in the former gel phase were now subsumed in the growing fluid phase.

It is interesting that the first stages of the gel to fluid phase transition occurred not at the preexisting defects but rather at what must be microscopic defects in the gel phase itself. This implies that the preexisting defects must be pinned, likely by disordered lipid adsorbed at the gel-defect interface. Moreover, the nucleating sites for the phase transition occurred at different locations on the surface during the reverse melting process (see below), which argues against a trivial explanation in terms of nucleation by impurities and dirt. The energy cost of freeing these adsorbed molecules must be greater than that required to "melt" other defects on the terrace. We note in Fig. 3(d) that the breakdown of the preexisting defect was not homogeneous, but rather occurred only at the gel-defect boundary. Those lipid molecules at the border of the defects, which were not well packed or adsorbed, transformed to the fluid phase. This is another indication that the boundary features an adsorbate with a distribution of adsorption energetics — i.e., disordered lipid molecules. Finally, the length of the interfacial boundary reached its maximum and the fluid domains coalesced and formed a continuous phase, resulting in decrease of the length. With subsequent temperature increase, the fluid phase continued to grow, coalesced into larger-and-larger islands, and eventually covered the entire surface [Fig. 3(f)]. Our experiments reveal the slow equilibration of the gel-to-LC phase transition, which is thermodynamically first order.

Figure 4 quantifies this and shows that the increase of fluid area followed first-order exponential growth. For a two-state system, we define α as the extent of transition; i.e., the fraction melted. According to the classical van't Hoff relationship [7], α can be expressed as a function of temperature, T, in the form

$$\ln\frac{\alpha}{1-\alpha} = -\frac{\Delta H_{vH}}{RT}, \tag{1}$$

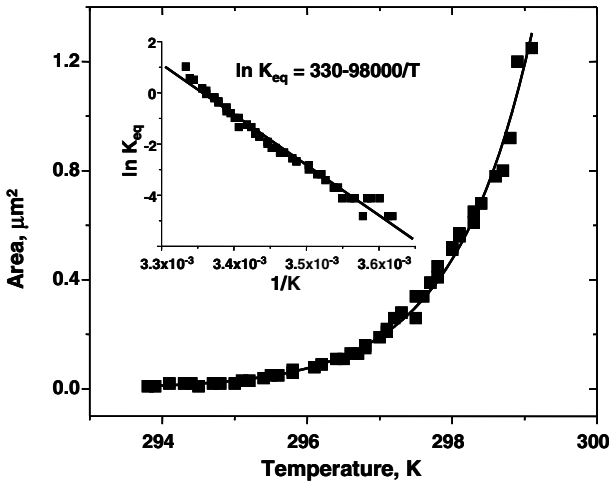

FIG. 4. Quantification of the phase transition. The area percentage of fluid phase is plotted as a function of increasing temperature. The solid line shows the fit to Eq. (1); the χ^2 parameter is 0.988 51. Inset: The fraction melted, K_{eq}, plotted as a function of $1/T$.

where ΔH_{vH} is the van't Hoff transition enthalpy. The inset of Fig. 4 shows our data agree well with this expression, where we define $K_{eq} \equiv \alpha/(1 - \alpha)$. Moreover, ΔH_{vH} follows from the slope of the line, $8.2 \pm 1 \times 10^5$ J mol^{-1}.

It is known that ideal melting is a perfectly cooperative process involving destruction of the infinite crystal lattice all at once and occurs over an infinitely narrow temperature range [7]. For substances with finite size, one can introduce the cooperative unit, N, to describe the number of identical entities within an ensemble. The enthalpy of the transition reported earlier from differential scanning calorimetry measurements is $\Delta H_t = 2.25 \times 10^4$ J mol^{-1} for vesicles of DMPC [16]. The ratio of ΔH_{vH} to ΔH_t gives N. In this case, $N = 35$–45. Tokumasu *et al.* [10] found an intrinsic domain size of 18–75, which is in a similar range. The small value may be caused by the finite ensemble size. As discussed above, the stress exerted on the bilayer during the phase transition decreases the size of cooperative domain.

Our analysis provides some insight into the mechanism of the gel-fluid phase transition. Interestingly, growth from the fluid nuclei was not isotropic, as might be expected for a uniform film, but rather showed considerable anisotropy with elongated fluid areas. The origin is likely strain in the gel phase, the tearing process described above. This suggests that absent an additional lipid in the solution above the fluid phase, the resultant gel phase will be strained as yet another consequence of the large density difference between the two phases [17]. The observation of anisotropic growth also strongly suggests that the fluid nuclei have their origin not in surface impurities but rather reflect stress in the gel film.

There are two kinds of phase growth evident. First, the fluid phase started to grow from the fluid nuclei. The second kind originated in the large preexisting defects. As the temperature was raised, large foamlike defects coalesced into islandlike structures, minimizing the perimeter of the interfacial boundary.

The significance of these findings is to call quantitative attention to defects and history of formation in the structure of supported lipid bilayers. The method of preparing the gel phase strongly affects the defect structure and this in turn has considerable impact on the subsequent gel to fluid phase transition. Gel phases prepared with insufficient lipid will feature large tearing defects and physical measurements following preparation will undoubtedly reflect the presence of these defects. Alternatively, these defects can be potentially useful as sites to modify the properties of supported bilayers through incorporation of additional constituents.

R. Y. was supported by the JSPS. This work was supported by the U.S. Department of Energy, Division of Materials Science under Award No. DEFG02-91ER45439 to the Frederick Seitz Materials Research Laboratory at the University of Illinois at Urbana-Champaign.

*Author to whom correspondence should be addressed. Electronic address: agewirth@uiuc.edu

†Author to whom correspondence should be addressed. Electronic address: sgranick@uiuc.edu

[1] A. A. Brian and H. M. McConnell, Proc. Natl. Acad. Sci. U.S.A. **81**, 6159 (1984).

[2] E. Sackmann, Science **271**, 43 (1996).

[3] S. G. Boxer, Curr. Opin. Chem. Biol. **4**, 704 (2000).

[4] P. S. Cremer and T. L. Yang, J. Am. Chem. Soc. **121**, 8130 (1999).

[5] M. M. Lipp, K. Y. C. Lee, D. Y. Takamoto, J. A. Zasadzinski, and A. J. Waring, Phys. Rev. Lett. **81**, 1650 (1998).

[6] B. Maier and J.O. Rädler, Phys. Rev. Lett. **82**, 1911 (1999).

[7] D. M. Small, in *The Physical Chemistry of Lipids* (Plenum Press, New York, 1986).

[8] L. K. Nielsen, T. Bjørnholm, and O. G. Mouritsen, Nature (London) **404**, 352 (2000).

[9] A. S. Muresan, H. Diamant, and K. Y. C. Lee, J. Am. Chem. Soc. **123**, 6951 (2001).

[10] F. Tokumasu, A. J. Jin, and J. A. Dvorak, J. Electron Microsc. **51**, 1 (2002).

[11] Z. Shao and J. Yang, Q. Rev. Biophys. **28**, 195 (1995).

[12] W. H. Han, S. M. Lindsay, and T. W. Jing, Appl. Phys. Lett. **69**, 4111 (1996).

[13] S. J. Johnson, T. M. Bayerl, D. C. McDermitt, G. W. Adam, A. R. Rennie, R. K. Thomas, and E. Sackmann, Biophys. J. **59**, 289 (1991).

[14] B. W. Koeing, H. H. Strey, and K. Gawrisch, Biophys. J. **73**, 1954 (1997).

[15] H. I. Petrache, S. Tristramnagle, and J. F. Nagle, Chem. Phys. Lipids **95**, 83 (1998).

[16] S. Mabrey and J. M. Sturtevant, Proc. Natl. Acad. Sci. U.S.A. **73**, 3862 (1976).

[17] We have preliminary evidence that having lipid in solution over the film can modify the pattern described above but the parameters of this are not simple.